Receptor-Mediated Pharmacokinetic/Pharmacodynamic Model of Interferon-β 1a in Humans

Donald E. Mager[1] and William J. Jusko[1,2]

Received April 2, 2002; accepted June 12, 2002

Purpose. An integrated receptor-based pharmacokinetic/pharmacodynamic (PK/PD) model of interferon-β 1a (IFN-β 1a) previously developed for monkeys was used to capture the time-course of drug and induced neopterin concentrations after intravenous (IV) and subcutaneous (SC) dosing in humans.

Methods. Data were extracted from the literature by digitalization. Single-dose (3 IV doses and 1 SC dose) PK/PD profiles were simultaneously fitted using the basic model and the ADAPT II computer program. Additional submodels incorporating neutralizing antibody formation and negative feedback inhibition were applied to account for drug accumulation and lower than expected neopterin concentrations encountered after multiple-dosing (1 SC dose every 48 hs).

Results. The basic model jointly-captured the nonlinear PK behavior of the drug and induced neopterin concentrations after all single doses. Slow and incomplete absorption (F = 0.33) of the SC dose resulted in prolonged drug concentrations reflective of flip-flop kinetics. Despite lower drug concentrations, SC dosing produced a similar neopterin profile as compared with the IV doses; however, with a longer time to peak effect and slightly higher neopterin concentrations at later time points. The PD component of the model represents a modified precursor-dependent indirect response model driven by the amount of internalized drug-receptor complex. The latter stimulated a 6-fold increase in the production of the neopterin precursor (S_{max} = 5.89). Drug accumulation and lower than expected neopterin concentrations after multiple dosing were also captured after the inclusion of the submodels.

Conclusions. The present integrated PK/PD model for IFN-β 1a is mechanistic in nature with receptor-mediated disposition and dynamics and was successfully applied to human clinical data.

KEY WORDS: interferon-beta; pharmacokinetics; pharmacodynamics; mathematical modeling; humans.

INTRODUCTION

Interferons (IFNs) are a family of endogenous type II cytokines with antiviral, antiproliferative, and immunomodulatory properties. Within this class of compounds, IFN-β is a subtype that has shown promise in the treatment of a variety of neoplastic and viral diseases and is currently being used in the treatment of multiple sclerosis (1). Although the exact mechanisms of action are still being investigated, the beneficial effects of IFN are thought to result from a combination of their biologic properties, which include: distributional changes of specific cells; activation of lymphocyte, macrophage, and natural killer cell cytotoxicity; regulation of cytokine and cytokine receptor gene expression; and an increase in expression of some tumor-associated antigens (2,3). More specifically, IFN-β has been shown to interact with a specific cellular membrane receptor and induce the production of several substances, such as neopterin, β2-microglobulin, 2′5′-oligoadenylate synthetase, and Mx-protein (3). Becaues these compounds are reflective of the cellular response to IFN-β, they have been found to be valuable biomarkers in clinical studies (4–7).

The connections between IFN-β pharmacokinetics (PKs) and subsequent pharmacodynamics (PDs) have not been well characterized thus far. Although previous studies have examined the influence of drug dose, formulation (4), and administration route (8) and frequency (7) on various responses to IFN-β, many of these studies were limited by the use of single-dose levels and/or noncompartmental analyses. To our knowledge, a mechanistic PK/PD model has not yet been published for IFN-β. Such a relationship may be of use in designing optimal dosing regimens and provide a means by which to further evaluate the role those system parameters may have in controlling net pharmacodynamic responses.

Recently, an integrated PK/PD model was presented (9), which simultaneously characterized the time-course of interferon-β 1a (IFN-β 1a) and induced neopterin plasma concentrations in monkeys after intravenous (IV) and subcutaneous (SC) dosing at various dose levels. Submodels were also included to account for elevated drug and lower-than-expected neopterin concentrations upon multiple dosing. In addition, we applied a general pharmacokinetic model of target-mediated drug disposition to characterize the time-course of IFN-β 1a plasma concentrations in humans after three IV bolus injections of 6, 12, and 18 million international units (MIU) (10). These models use receptor binding and subsequent internalization (receptor-mediated endocytosis) as the primary mechanism of drug elimination, and well capture the nonlinear PK behavior of the drug. The purpose of this report is to determine whether the former integrated PK/PD approach could be extended to jointly characterize the time-course of IFN-β 1a serum concentrations after IV and SC dosing, as well as their inductive effects on serum neopterin concentrations in humans (11).

METHODS

Data Source

Mean PK/PD data were extracted from a study conducted by Buchwalder *et al.* (11). In one study panel, three increasing IV bolus doses (6, 12, and 18 MIU) of IFN-β 1a were given to healthy volunteers (four female and four male) at 1-week intervals. In a second panel, 18 MIU was administered to healthy volunteers (six female and six male) by intramuscular, IV, and SC injection (crossover design at 1-week intervals). Multiple dosing was evaluated in the final study panel, where four SC doses of 18 MIU were given at 48-h intervals to four male and four female volunteers. The IFN-β 1a and neopterin concentration-time data were recaptured by computer digitalization (Sigma Scan, Jandel Scientific, Corte Madera, CA, USA).

[1] Department of Pharmaceutical Sciences, School of Pharmacy and Pharmaceutical Sciences, University at Buffalo, State University of New York, 565 Hochstetter Hall, Buffalo, New York 14260.

[2] To whom correspondence should be addressed. (e-mail: wjjusko@acsu.buffalo.edu)

PK/PD Model

The fully integrated PK/PD model is shown in Fig. 1 (bracketed components represent submodels used to characterize multiple dosing). The pharmacokinetic component for IV dosing (D_{IV}) has been described elsewhere (10). Briefly, drug in the serum or central compartment (D_P, Vc) is eliminated from the system through receptor-mediated endocytosis (3). This process is reflected in the model as an interaction with free receptors (R_f) to form a drug-receptor complex (DR) via reversible (k_{on} and k_{off}) binding, followed by cellular internalization (k_m). The limited quantity of total receptors (R_{max}) creates nonlinear elimination. The use of a time-independent R_{max} parameter assumes a constant total cell-surface density of receptors, the validity of which has been discussed (10). Literature suggests that internalized receptors are not recycled to the cell surface (12) and was thus not incorporated into the model. A tissue compartment (D_T) with linear first-order distribution processes (k_{pt} and k_{tp}) was used to account for nonspecific drug binding. Although secondary elimination pathways have been identified for IFN-β, preliminary data fitting showed that the inclusion of these processes were unnecessary (10).

The SC absorption of IFN-β 1a was modeled using a modified approach of Radwanski *et al.* (13). Delayed and prolonged absorption is often observed for relatively large macromolecules (IFN-β MW ~20,000) because of lymphatic uptake from SC injection sites (14). This input mechanism is shown in Fig. 1 as linear first-order absorption (ka) from the injection site into a lymph compartment (D_L), followed by uptake into the systemic circulation (ka2). A bioavailability parameter (Bio) was also included to account for incomplete drug absorption.

The differential equations used to describe IFN-β 1a pharmacokinetics were as follows:

$$\frac{dD_{P,iv}}{dt} = k_{tp} \cdot D_{T,iv} - k_{pt} \cdot D_{P,iv} - \left(\frac{k_{on}}{Vc}\right) \cdot D_{P,iv} \cdot R_{f,iv} + k_{off} \cdot DR_{iv} \quad (1)$$

$$\frac{dD_{P,sc}}{dt} = ka2 \cdot D_L + k_{tp} \cdot D_{T,sc} - k_{pt} \cdot D_{P,sc} - \left(\frac{k_{on}}{Vc}\right) \cdot D_{P,sc} \cdot R_{f,sc} + k_{off} \cdot DR_{sc} \quad (2)$$

$$\frac{dDR_{ad}}{dt} = \left(\frac{k_{on}}{Vc}\right) \cdot D_{P,ad} \cdot R_{f,ad} - (k_{off} + k_m) \cdot DR_{ad} \quad (3)$$

$$\frac{dD_{T,ad}}{dt} = k_{pt} \cdot D_{P,ad} - k_{tp} \cdot D_{T,ad} \quad (4)$$

$$\frac{dD_L}{dt} = ka \cdot Bio \cdot D_{sc} \cdot e^{-ka \cdot t} - ka2 \cdot D_L \quad (5)$$

$$R_{f,ad} = R_{max} - DR_{ad} \quad (6)$$

where *ad* represents the route of administration (IV or SC) and the symbols are defined previously. Serum IFN-β 1a concentrations were set equal to $D_{P,iv}/Vc$ and $D_{P,sc}/Vc$ for IV and SC doses (nM units were converted to IU/mL). The initial condition for Eq. (1) was D_{IV} whereas Equations 2–5 were initially set to zero.

The pharmacodynamic biomarker was serum neopterin concentrations (NP), the biosynthetic pathway of which is shown in Fig. 2. IFN-β is thought to stimulate neopterin production through induction of the guanosine triphosphate-cyclohydrolase I enzyme (15). Once formed, neopterin does not appear to be a substrate for conjugation or metabolism and is primarily eliminated by renal excretion (15). A modified precursor-dependent indirect pharmacodynamic response model (16) was proposed to characterize the time-course of serum neopterin concentrations and is also shown in Fig. 1. Internalized drug-receptor complex (DR*) was used to

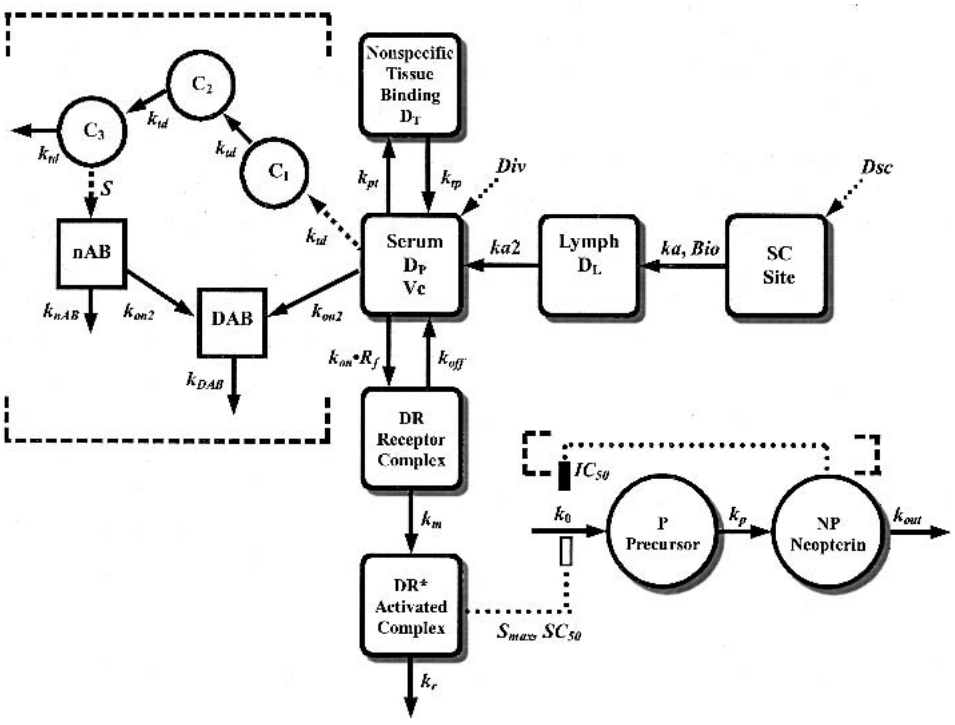

Fig. 1. Proposed pharmacokinetic-pharmacodynamic model for IFN-β 1a.

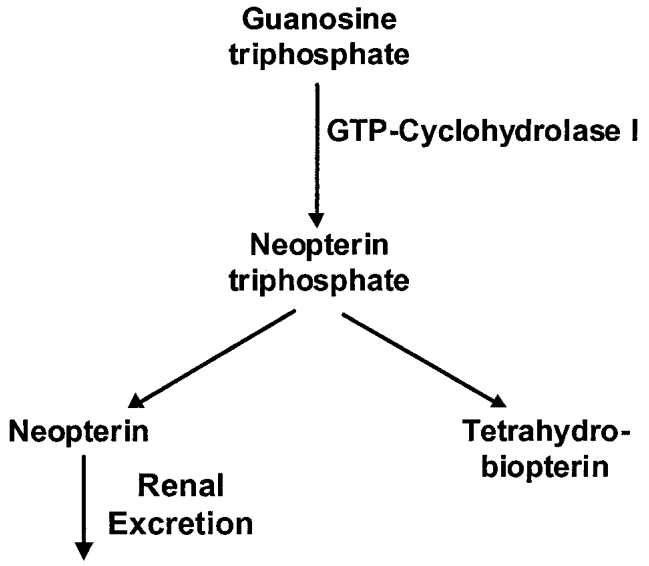

Fig. 2. Biosynthetic pathway of neopterin (adapted from Reference 15).

stimulate the apparent zero-order production rate (k_0) of the neopterin precursor (P; neopterin triphosphate), which in turn was responsible for the production (k_p) of the pharmacodynamic response variable (NP; neopterin). The rate of change of DR* over time can be represented by:

$$\frac{dDR^*_{ad}}{dt} = k_m \cdot DR_{ad} - k_r \cdot DR^*_{ad} \quad (7)$$

where DR and k_m are controlled by the pharmacokinetics and the first-order loss of DR* (k_r) by the dynamics. The initial conditions were set to zero. The resulting DR* profiles were used to stimulate precursor production as:

$$\frac{dP_{ad}}{dt} = k_0 \cdot \left(1 + \frac{S_{max} DR^*_{ad}}{SC_{50} + DR^*_{ad}}\right) - k_p \cdot P_{ad} \quad (8)$$

The stimulation function is governed by capacity (S_{max}) and sensitivity (SC_{50}) parameters, whereas the conversion to neopterin is modeled using a first-order rate constant (k_p). Thus, the formation and loss of neopterin can be defined by:

$$\frac{dNP_{ad}}{dt} = k_p \cdot P_{ad} - k_{out} \cdot NP_{ad} \quad (9)$$

where k_{out} is the first-order elimination rate of the response variable and the initial condition is equal to the average zero-time response (NP^0). Because stationarity is assumed, the zero-order production rate of the precursor was defined as:

$$k_0 = k_{out} \cdot NP^0 \quad (10)$$

thus reducing the number of parameters to be estimated. Likewise, the initial concentration of precursor (P^0) can be determined (16) from the ratio of its production and loss:

$$P^0 = k_0/k_p \quad (11)$$

Multiple Dosing

The pharmacokinetic profile of IFN-β 1a following multiple dosing was characterized using a modified neutralizing antibody (nAB) submodel (17) and is shown on the left side of Fig. 1 (bracketed components). A series of three delay compartments accounted for the time-lag of nAB formation,

$$dC_1/dt = k_{td} \cdot (D_{P,sc} - C_1) \quad (12)$$

$$dC_2/dt = k_{td} \cdot (C_1 - C_2) \quad (13)$$

$$dC_3/dt = k_{td} \cdot (C_2 - C_3) \quad (14)$$

where C_n is the amount in the n^{th} delay compartment and k_{td} is a first-order rate constant. The dashed arrow leading to the first delay compartment indicates that this process is assumed to not affect the pharmacokinetics of D_P. Formation of nAB is driven by a linear stimulation function driven by C_3 as,

$$\frac{dnAB}{dt} = S \cdot C_3 - k_{nAB} \cdot nAB \quad (15)$$

where S is a pseudo-first-order stimulation constant and k_{nAB} is a first-order rate constant of nAB elimination. Finally, the time course of the drug-nAB (DAB) complex can be described by the following equation,

$$\frac{dDAB}{dt} = k_{on2} \cdot D_P \cdot nAB - k_{DAB} \cdot DAB \quad (16)$$

where k_{on2} is a second-order formation rate constant and k_{DAB} is the first-order elimination rate of the DAB complex. This process clearly alters D_P kinetics and thus Eq. (2) was modified to reflect the apparent irreversible binding of drug to nAB. Total drug concentrations were modeled as the sum of DAB and D_P per volume of the central compartment (Vc).

Lower than expected neopterin concentrations after multiple dosing was accomplished with a submodel of negative feedback inhibition (Fig. 1; right side bracketed components). The submodel of nAB formation was fixed and the neopterin feedback was characterized by an indirect response (18) as defined by the following differential equation,

$$\frac{dS_{max}}{dt} = k_{out2} \cdot S^0_{max} \left(1 - \frac{NP}{IC_{50} + NP}\right) - k_{out2} \cdot S_{max} \quad (17)$$

where S^0_{max} is the value of S_{max} determined from the single-dose fitting, k_{out2} is the apparent first-order dissipation of S_{max}, and IC_{50} is the concentration of neopterin (NP) producing 50% inhibition of the theoretical formation rate of S_{max}.

Data Analysis

The proposed model (Fig. 1) was fitted to the single-dose data using a three-stage approach. In the first stage, IFN-β 1a concentration-time data after IV and SC dosing were fitted using Equations 1 – 6. The estimated parameters from simultaneous fitting included k_{pt}, k_{tp}, k_{on}, k_{off}, k_m, Vc, R_{max}, Bio, ka, and ka2. The initial estimate of Bio was calculated as the ratio of the area under the concentration curves (AUC_{SC}/AUC_{IV}), whereas ka was estimated using the Area Function Method (19). It was assumed that the second absorption rate constant (ka2) would be at least 5-fold greater than ka. For the remaining PK parameters, the previously reported parameter values were used as initial estimates (10).

The second-stage involved fixing the PK profiles from the first-stage as driving functions for the pharmacodynamic responses. Response-time data were simultaneously fitted us-

ing Eqs. (7–11), and the estimated parameters were S_{max}, SC_{50}, k_{out}, k_p, and k_r. Initial parameter estimates were calculated as described elsewhere (16,18).

In the final stage, all single-dose PK/PD data were jointly modeled using the fully integrated model (Eqs. [1–11]; Fig. 1), with values from the first two stages as initial estimates. The second stage of the analysis suggested that the SC_{50} value could be represented as the equilibrium dissociation constant for the drug-receptor complex:

$$SC_{50} = \frac{k_{off}}{k_{on}} \cdot Vc \tag{18}$$

and thus further reduced the number of system parameters. The final estimated parameters were fixed for estimating the PK/PD parameters associated with the submodels for multiple dosing (k_{td}, S, k_{nAB}, k_{DAB}, k_{out2}, and IC_{50}). The value of k_{on2} was assumed to be equal to k_{on} to further reduce the number of parameters.

All parameters were estimated using the ADAPT II computer program (20) by the maximum likelihood method. The variance models were defined as:

$$VAR_i = \sigma_1^2 \cdot M(\theta, t_i)^{\sigma 2} \tag{19}$$

where VAR_i is the variance of the i^{th} data point, σ_1 and σ_2 are the vectors of variance parameters ($\sigma_2 = 2$), and $M(\theta,t_i)$ is the ith predicted value from the PK/PD model. The goodness-of-fit was assessed by system convergence, Akaike Information Criterion, Schwartz Criterion, estimator criterion value for the maximum likelihood method in ADAPT II, correlation coefficients (R^2), examination of residuals, and visual inspection.

RESULTS

Pharmacokinetics

The time-course of mean IFN-β 1a plasma concentrations after three IV doses and one SC dose is shown in Fig. 3.

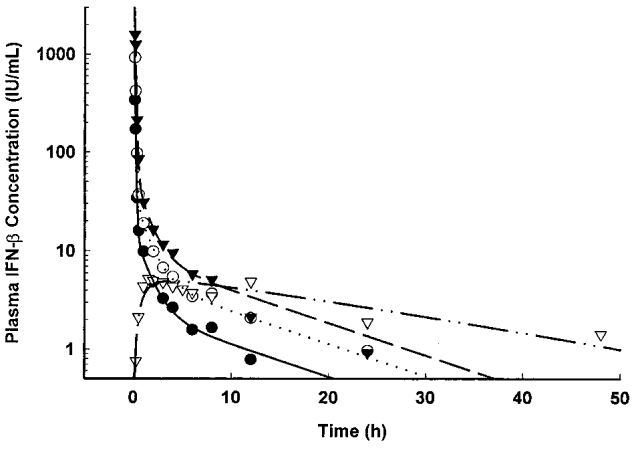

Fig. 3. Time-course of mean interferon-β 1a plasma concentrations after single dosing. The symbols represent data extracted from Reference 11, and the lines are model predicted profiles after the simultaneous fitting of all PK/PD data (stage 3 in the Methods section). Doses are 6 MIU IV (●; solid line), 12 MIU IV (○; dotted line), 18 MIU IV (▼; dashed line), and 18 MIU SC (▽; dash-dot-dot line).

Whereas the IV profiles exhibit polyexponential behavior, with steep distribution phases and more prolonged terminal phases, the SC profile appears biphasic, with concentrations still detectable after 40 h.

The proposed model well captures the pharmacokinetics after both routes of administration, and the model fitted curves are shown in Fig. 3. The final estimated parameters are listed in Table I, and the relatively low CV% values are also indicative of good model performance. The estimated volume of the central compartment (3.61 L) approximates plasma volume, suggesting that the relatively large compound (MW ~20,000) resides primarily within the vascular compartment. An equilibrium dissociation constant may be calculated (KD $= k_{off}/k_{on} = 0.1 \times 10^{-10}$ M), which falls within the reported range for IFN-β 1a and its biologic receptor (3).

Incomplete absorption occurs after SC dosing (Bio = 0.33), with peak concentrations of about 5 IU/mL around 4 h after administration. The estimated value of the first-order absorption rate constant (ka) was 0.0414 h^{-1}, and is slower than the second absorption rate constant (ka2) of 1.25 h^{-1}. The prolonged plasma concentrations after SC dosing and relatively slow absorption are indicative of flip-flop kinetics.

Pharmacodynamics

Mean neopterin plasma concentrations after the IV and SC dosing of IFN-β 1a are shown in Fig. 4. These profiles demonstrate a delayed onset and a slow return toward baseline levels, consistent with the indirect mechanism of action of IFN-β 1a.

The modified precursor-dependent indirect response model appears to reasonably capture the time-course of neopterin concentrations (Fig. 4). Final estimated parameters are

Table I. Estimated Pharmacokinetic and Pharmacodynamic Parameters

Parameter (units)	Final estimate	CV%
Pharmacokinetic parameters		
k_{pt} (h^{-1})	2.18	7.7
k_{tp} (h^{-1})	0.0928	11
k_{off} (h^{-1})	0.111	15
k_{on} ($nM^{-1}h^{-1}$)	8.71	19
k_m (h^{-1})	0.707	15
Vc (L)	3.61	13
R_{max} (nmol)	4.95	16
ka (h^{-1})	0.0414[a]	8.2
ka2 (h^{-1})	1.25[a]	18
Bio	0.330	8.8
Pharmacodynamic parameters		
S_{max}	5.89	20
k_{out} (h^{-1})	0.253	50
k_p (h^{-1})	0.0466	21
k_r (h^{-1})	0.118	29
SC_{50} (nmol)	0.0460[b]	—[c]
P^0 (nM)	36.7[d]	—[c]
k_0 (nM/h)	1.71[e]	—[c]

[a] Parameters lack sufficient identifiability and are interchangeable (see Discussion).
[b] Secondary parameter calculated as: $SC_{50} = k_{off}/k_{on} \cdot Vc$.
[c] Not applicable.
[d] Secondary parameter calculated as: $P^0 = k_0/k_p$.
[e] Secondary parameter calculated as: $K_0 = NP^0 \cdot k_{out}$.

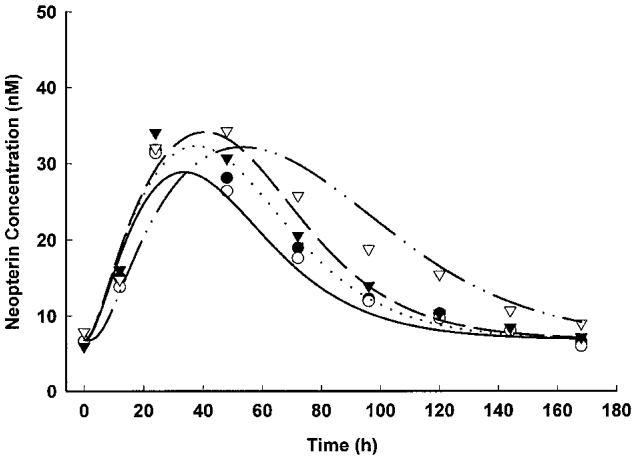

Fig. 4. Time-course of mean neopterin plasma concentrations after single dosing. The symbols represent data extracted from Reference 11, and the lines are jointly model predicted profiles. Doses are as in Fig. 3.

listed in Table I. The internalized drug-receptor complex seems to be responsible for a 6-fold increase (S_{max} = 5.89) in the zero-order production rate (k_0) of the precursor. The half-life of neopterin can be calculated from its elimination rate constant as, ln(2) / k_{out} = 2.7 h, which is similar to the reported value of 1.5 h (21).

Multiple Dosing

The mean pharmacokinetic profile of IFN-β 1a after multiple-dosing (18 MIU SC every 48 h for 4 doses) shows gradual drug accumulation and a more prolonged elimination phase after the last dose as compared with the first dose (Fig. 5). A simulation of the PK component of the basic model (Eqs. [2–6], Table I) failed to demonstrate these characteristics (data not shown). A modified neutralizing antibody submodel was applied and well captured the major features of the data (Fig. 5). The final estimated parameters were: k_{td} = 0.129 h^{-1} (22 CV%), S = 0.534 (16 CV%), k_{nAB} = 0.237 h^{-1} (15 CV%), and k_{DAB} = 0.00634 h^{-1} (13 CV%).

The equations and model parameters for the multiple-dosing pharmacokinetic profile were fixed, and a simulation of the pharmacodynamics was conducted (dashed line in Fig. 6). Despite the incorporation of the neutralizing antibody submodel, the predictions failed to describe the lower than expected neopterin concentrations after multiple dosing (Fig. 6). A submodel incorporating principles of negative feedback inhibition, driven by neopterin concentrations, sufficiently attenuated the multiple-dosing response profile (solid line in Fig. 6). The estimated pharmacodynamic parameters were: IC_{50} = 3.67 nM (146 CV%) and k_{out2} = 0.00680 h^{-1} (37 CV%).

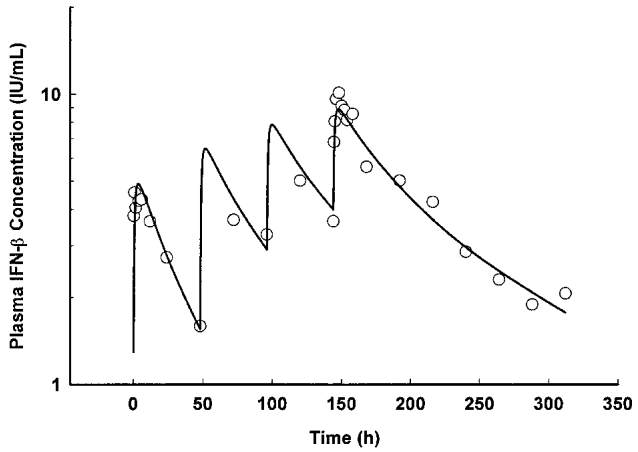

Fig. 5. Time-course of mean interferon-β 1a plasma concentrations after 18 MIU SC every 48 h for four doses. Symbols represent data extracted from Reference 11. The solid line is the profile resulting from fitting of the neutralizing antibody submodel.

DISCUSSION

Therapeutic cytokines are rapidly developing into a large class of drugs with considerable clinical potential. These endogenous proteins are often ligands for highly specific biologic receptors. In addition to the pharmacodynamic implications, this interaction with high affinity target sites can have a significant role in the disposition of these drugs (22). Thus, the potential exists for target-mediated drug disposition, where the binding of drug to its pharmacologic target is significant (relative to dose) and reflected in its pharmacokinetic characteristics (23). The most typical manifestation is a dose-dependent apparent volume of distribution when assessed by area/moment analysis. However, when target binding is also implicated in elimination (e.g., receptor-mediated endocytosis), nonlinear systemic clearance may also occur. Although only the change in IFN-β 1a clearance with increasing doses was statistically significant, both the apparent volume of distribution and clearance of IFN-β 1a decreased with increasing dose levels as determined by a noncompartmental analysis (11). The final PK/PD model (Fig. 1) accommodates these attributes in a mechanistic manner and well-captured IFN-β 1a profiles after single IV and SC doses (Fig. 3). Furthermore, the Vc matching the plasma volume and the k_{off}/k_{on} reflecting the equilibrium dissociation constant add a degree of physiologic significance to the model.

The SC administration of IFN-β 1a produced lower drug

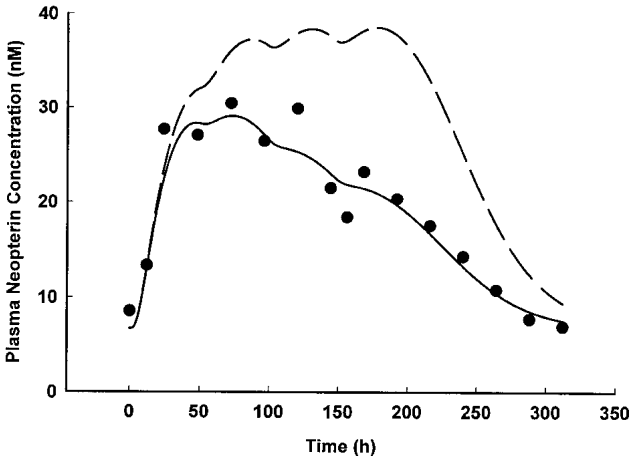

Fig. 6. Time-course of mean neopterin concentrations after 18 MIU of inteferon-β 1a SC every 48 h for four doses. Symbols are data extracted from Reference 11. Lines are the predictions of the PD model after incorporating the neutralizing antibody submodel alone (dashed line) or in combination with fitting the negative feedback submodel (solid line).

concentrations, incomplete bioavailability, and flip-flop PK behavior. The estimated bioavailability (33%) is in good agreement with the previously determined value of 27% by noncompartmental analysis (11). The absorption characteristics were described by drug transport into a lymphatic compartment, followed by absorption into the central plasma compartment. However, the values of the two absorption rate constants (ka and ka2) must be interpreted with caution. The true transport characteristics between these compartments are not discernible from just plasma concentration data, and simulations show that the values of ka and ka2 are interchangeable (data not shown). Regardless, the slower of the two rate constants will represent the rate-limiting process in the SC absorption of the drug.

The final single-dose PK/PD model (Fig. 1) also characterized the time-course of induced neopterin concentrations following both routes of drug administration (Fig. 4), and is mechanistically consistent with IFN-β pharmacology. The main pathways of IFN-α/β signaling have been reviewed elsewhere (24). In our model, the internalization rate constants (k_m and k_r) may be viewed as establishing a transit compartment (DR*) reflective of the time required for these cellular processes to occur. The DR* signal is then used to stimulate the production of the neopterin precursor using a precursor-dependent indirect response model (16), consistent with neopterin turnover (Fig. 2). Interestingly, despite the lower drug concentrations after SC dosing, the model sufficiently captured the similar resulting neopterin profile, and included an apparent later time to peak effect and slightly elevated neopterin concentrations at later time points (Fig. 4). This may be attributable to nonlinear drug binding, which is responsible for both drug elimination as well as initiating the signal for neopterin stimulation, in conjunction with the role of slow drug absorption. Whereas traditional PK/PD models are often developed using a separation principle where kinetics are determined and fixed for subsequent PD fitting, the approach presented in this study uses simultaneous modeling of all PK/PD data. The intimate relationship between the mechanisms of drug disposition and pharmacologic effect justifies this methodology and is further reflected in the use of a single SC_{50}-K_D parameter.

These PK/PD properties are qualitatively similar to those observed for monkeys (9). However, the doses given to the monkeys were considerably larger (1 to 10 MIU/kg for monkeys vs. 0.09 to 0.3 MIU/kg for humans). The larger doses are most likely responsible for some species differences. For example, a secondary elimination pathway was required in the basic PK/PD model for monkeys. With higher doses, the primary elimination route is most likely saturated, which would sustain drug concentrations and increase the likelihood of alternate elimination mechanisms such as renal catabolism or proteolytic degradation. Also, whereas the bioavailability of the lower SC doses in monkeys was comparable with that in humans, the largest dose in monkeys (10 MIU/kg) resulted in a much higher estimated value (about 80%). Again, the higher SC dose may have resulted in saturation of drug catabolism at the SC site resulting in a nonlinear or dose-dependent bioavailability. The PD profiles after single doses in monkeys were clearly dose dependent whereas the study in humans suggests a greater degree of saturation (Fig. 4), at least for the given dose range. Despite these quantitative differences, the basic model can be applied to PK/PD data from both species, and monkeys appear to be a suitable pre-clinical animal model for IFN-β 1a kinetics and dynamics. The central volume of distribution reflecting plasma volume and the ability to use a similar SC_{50}-K_D parameter were observed for both species.

Repeated SC administration of IFN-β 1a resulted in drug accumulation (Fig. 5) and lower than expected neopterin concentrations (Fig. 6) at later doses, which could not be accounted for by the basic PK/PD model. These observations upon multiple dosing have been reported in clinical studies (7) and were also seen in monkeys (9). In that study, drug accumulation was hypothesized to result from receptor down-regulation and was successfully modeled using a submodel as defined by the following differential equation:

$$\frac{dR_{max}}{dt} = k_{syn,R_{max}} \cdot \left(1 - \frac{DR^*}{IC_{50,R_{max}} + DR^*}\right) - k_{deg,R_{max}} \cdot R_{max} \quad (20)$$

where the initial condition, R^0_{max}, is the R_{max} value estimated from single-dose data and $k_{syn,Rmax}$ is the theoretical zero-order synthesis rate of total receptor density, defined as the product of the first-order degradation rate ($k_{deg,Rmax}$) and R^0_{max}. However, the terminal phase of the drug after the last dose was parallel to that after the initial dose. Although applying this approach to the human data captured the peak concentrations of the last dose, it failed to account for the trough concentrations before the third and fourth dose as well as the prolonged drug concentrations after the fourth dose (data not shown). A down-regulation of the internalization constant (k_m) was also applied and, although this improved the overall fitting to the multiple-dose PK data, these prolonged drug concentrations produced elevated and sustained neopterin concentrations (as described by Eqs. [8–11]) that are inconsistent with the data. This may imply that whatever mechanisms are causing the increased drug concentrations do so in a manner by which these concentrations are not "seen" by the cell-surface receptors. Therefore, we hypothesized that neutralizing antibodies may have formed, complexed with free drug, and sustained total drug concentrations while reducing available concentrations for binding with receptors. A modified neutralizing antibody model was applied (17) and resulted in the best fitting of the multiple-dose PK data (Fig. 5). It is important to note that neutralizing antibodies were not observed in the previously mentioned clinical study (7), more time may be required for such antibodies to form, and that neutralizing antibodies form with a much lower incidence with IFN-β 1a than with IFN-β 1b (21). Despite the inclusion of this submodel, neopterin concentrations were still lower than simulated responses after multiple-dosing (dashed line in Fig. 6). Lower neopterin concentrations have been reported in the literature (7,21) and were observed in the monkey study (9). A negative feedback mechanism was proposed in the previous monkey study and in this present analysis which well-described the resulting multiple-dose PD profile (Fig. 6). In a previous clinical study by Liberati *et al.* (25), patients with higher baseline neopterin concentrations had lower than expected profiles of neopterin (with some even exhibiting decreased values) after IFN-β administration. This suggests that higher neopterin concentrations may inhibit the ability of IFN-β 1a to induce neopterin production and supports the proposed submodel (Eq. 17).

In conclusion, an integrated PK/PD model of IFN-β 1a has been successfully applied to human clinical data. The proposed model is mechanistic in nature, attempting to include the major pharmacologic processes involved in both drug kinetics and dynamics. Although submodels were included to account for additional complexities upon multiple dosing, further research is required to assess their validity and role in designing appropriate drug dosing regimens.

ACKNOWLEDGMENTS

This work was supported in part by NIH Grant GM57980 and a Pre-doctoral Fellowship for DEM from the American Foundation for Pharmaceutical Education.

REFERENCES

1. J. H. Noseworthy, C. Lucchinetti, M. Rodriguez, and B. G. Weinshenker. Multiple sclerosis. *N. Engl. J. Med.* **343**:938–952 (2000).
2. W. Leonard. Type I cytokines and interferons and their receptors. In W. Paul (ed.), *Fundamental Immunology,* Lippincott-Raven, Philadelphia, Pennsylvania, 1999 pp. 741–774.
3. S. Pestka, J. A. Langer, K. C. Zoon, and C. E. Samuel. Interferons and their actions. *Annu. Rev. Biochem.* **56**:727–777 (1987).
4. J. Alam, S. Goelz, P. Rioux, J. Scaramucci, W. Jones, A. McAllister, M. Campion, and M. Rogge. Comparative pharmacokinetics and pharmacodynamics of two recombinant human interferon beta-1a (IFN beta-1 a) products administered intramuscularly in healthy male and female volunteers. *Pharm. Res.* **14**:546–549 (1997).
5. J. Chiang, C. A. Gloff, C. N. Yoshizawa, and G. J. Williams. Pharmacokinetics of recombinant human interferon-beta ser in healthy volunteers and its effect on serum neopterin. *Pharm. Res.* **10**:567–572 (1993).
6. G. Fierlbeck, A. Ulmer, T. Schreiner, W. Stroebel, U. Schiebel, and J. Brzoska. Pharmacodynamics of recombinant IFN-beta during long-term treatment of malignant melanoma. *J. Interferon Cytokine Res.* **16**:777–781 (1996).
7. L. E. Rothuizen, T. Buclin, F. Spertini, I. Trinchard, A. Munafo, P. A. Buchwalder, A. Ythier, and J. Biollaz. Influence of interferon beta-1a dose frequency on PBMC cytokine secretion and biologic effect markers. *J. Neuroimmunology* **99**:131–141 (1999).
8. P. Salmon, J. Y. Le Cotonnec, A. Galazka, A. Abdul-Ahad, and A. Darragh. Pharmacokinetics and pharmacodynamics of recombinant human interferon- beta in healthy male volunteers. *J. Interferon Cytokine Res.* **16**:759–764 (1996).
9. D. E. Mager, B. Neuteboom, A. Murafo, C. Efthymiopoulos, and W. J. Jusko. Receptor-mediated pharmacokinetics and pharmacodynamics of IFN-beta 1a following intravenous and subcutaneous dosing in monkeys. In *Pharmaceutical Congress of the Americas*. AAPS, Orlando, Florida, 2001.
10. D. E. Mager and W. J. Jusko. General pharmacokinetic model for drugs exhibiting target-mediated drug disposition. *J. Pharmacokinet. Pharmacodyn.* **28**:507–532 (2001).
11. P. A. Buchwalder, T. Buclin, I. Trinchard, A. Munafo, and J. Biollaz. Pharmacokinetics and pharmacodynamics of IFN-beta 1a in healthy volunteers. *J. Interferon Cytokine Res.* **20**:857–866 (2000).
12. K. C. Zoon and H. Arnheiter. Studies of the interferon receptors. *Pharmacol. Ther.* **24**:259–278 (1984).
13. E. Radwanski, A. Chakraborty, S. Van Wart, R. D. Huhn, D. L. Cutler, M. B. Affrime, and W. J. Jusko. Pharmacokinetics and leukocyte responses of recombinant human interleukin-10. *Pharm. Res.* **15**:1895–1901 (1998).
14. A. Supersaxo, W. Hein, and H. Steffen. Effect of molecular weight on the lymphatic absorption of water-soluble compounds following subcutaneous administration. *Pharm. Res.* **7**:167–169 (1990).
15. D. Fuchs, G. Weiss, G. Reibnegger, and H. Wachter. The role of neopterin as a monitor of cellular immune activation in transplantation, inflammatory, infectious, and malignant diseases. *Crit. Rev. Clin. Lab. Sci.* **29**:307–341 (1992).
16. A. Sharma, W. F. Ebling, and W. J. Jusko. Precursor-dependent indirect pharmacodynamic response model for tolerance and rebound phenomena. *J. Pharm. Sci.* **87**:1577–1584 (1998).
17. R. Braeckman. Pharmacokinetics and pharmacodynamics of protein therapeutics. In R. E. Reid (ed.), *Peptide and Protein Drug Analysis,* University of British Columbia, Vancouver, 1999 pp. 633–669.
18. N. L. Dayneka, V. Garg, and W. J. Jusko. Comparison of four basic models of indirect pharmacodynamic responses. *J. Pharmacokinet. Biopharm.* **21**:457–478 (1993).
19. H. Cheng, A. Staubus, and L. Shum. An area function method for estimating the apparent absorption rate constant. *Pharm. Res.* **5**:57–60 (1988).
20. D. Z. D'Argenio and A. Schumitzky. ADAPT II user's guide. Biomedical Simulations Resource, Los Angeles, California, 1997.
21. S. D. Cook, J. R. Quinless, A. Jotkowitz, P. Beaton, and the Neutralizing Antibody Study Group. Serum IFN neutralizing antibodies and neopterin levels in a cross-section of MS patients. *Neurology* **57**:1080–1084 (2001).
22. Y. Sugiyama and M. Hanano. Receptor-mediated transport of peptide hormones and its importance in the overall hormone disposition in the body. *Pharm. Res.* **6**:192–202 (1989).
23. G. Levy. Pharmacologic target-mediated drug disposition. *Clin. Pharmacol. Ther.* **56**:248–252 (1994).
24. G. Stark, I. Kerr, B. Williams, R. Silverman, and R. Schreiber. How cells respond to interferons. *Annu. Rev. Biochem.* **67**:227–264 (1998).
25. A. M. Liberati, M. Fizzotti, M. G. Proietti, R. Di Marzio, M. Schippa, B. Biscottini, M. Senatore, P. Berruto, S. Canali, G. Peretti, and G. Zanolo. Biochemical host response to interferon-beta. *J. Interferon Res.* **8**:765–777 (1988).